PAPER Nr. : 12

RADIAL DISTRIBUTION CIRCULATION OF A ROTOR IN HOVER MEASURED BY LASER VELOCIMETER

BY

M. NSI MBA, C. MEYLAN, C. MARESCA, D. FAVIER

INSTITUT DE MECANIQUE DES FLUIDES DE MARSEILLE
LA 03 DU C.N.R.S.
1, rue Honnorat - 13003 MARSEILLE, FRANCE

TENTH EUROPEAN ROTORCRAFT FORUM

AUGUST 28 – 31, 1984 – THE HAGUE, THE NETHERLANDS

RADIAL DISTRIBUTION CIRCULATION OF A ROTOR IN HOVER MEASURED BY LASER VELOCIMETER

by

M. NSI MBA, C. MEYLAN, C. MARESCA, D. FAVIER

Institut de Mécanique des Fluides de Marseille
LA 03 du C.N.R.S.
1, rue Honnorat - 13003 MARSEILLE, FRANCE

ABSTRACT. A laser velocimeter was used to determine the circulation by integration of the velocity vector along a contour surrounding the blade section of a helicopter in hover. Two different contours were tested and compared. The radial distribution of circulation were then measured for rotors of different tip shape (rectangular, parabolic, tapered, swept) and presented comparatively to numerical results based on a free wake analysis code.

NOTATION.

b =	number of blades	
c =	local blade chord	: m
C_l =	local lift coefficient	: $2\,\Pi/c(\Omega r)$
C_T =	thrust coefficient	: $T/\rho(\Omega R)^2 \times \Pi R^2$
ℓ =	rotor blade loading per unit length	: N
T =	rotor thrust	: N
r =	local radial position	: m
R =	rotor radius	: m
U =	tangentiel velocity	: ms^{-1}
W =	axial velocity	: ms^{-1}
Γ =	bound circulation	: $m^2 s^{-1}$
$\theta_{0,75}$ =	blade pitch at 0,75 R	: d°
σ =	rotor solidity : $\frac{bc}{\Pi R}$	
ψ =	azimuthal of a blade	: d°
Ω =	rotor rotational speed	: rad s^{-1}

1. INTRODUCTION.

In order to improve the rotorcraft hover performance, several numerical procedures predicting the wake geometry, the rotor inflow and blade loading have been developped (see for instance the proceedings of the last European Rotorcraft Forum, Aerodynamics Session [(1)]. The validation of these codes is made by comparison with data available on the rotor induced flow field (wake geometry and velocities measurement [(2) (3)]) and on total rotor lift and load distribution. Some discrepancies have raised concerning measured and predicted tip vortex path and velocity distribution in the wake for particular twist and tip shape of the blades. Most of the existing codes are based on iterative calculation made on the radial bound circulation of the blade. A precise measurement of this quantity has been lacking as long as the use of the laser velocimeter was introduced[(4)] and made possible a non intrusive investigation of the bound circulation distribution. Probe interference and eventual encounters when measurements are performed close to the blades can then be avoided. Moreover, the influence of the tailoring of blade tip - plan forms on circulation distribution in the tip region can be rapidely infered and documented; such results present practical applications in the fields of aerodynamics and acoustics and aeroelasticity.

The present paper aims to carry out some new experimental results in the field and compare them to calculations deduced from a free wake analysis code[(5)] . Two original techniques for circulation measurements have been used and compared.

One of them consists in determining by use of a 2.D laser velocimeter, operating in backscattering mode, the velocity tangent to a close rectangular box surrounding the airfoil section at different radial locations of the blade. The measurement volume is displaced all along the box and the circulation is then calculated by curvilinear integration of measured velocities realised at the same phase corresponding to a position of the blade airfoil inside the box.

The other technique, owing the symmetry of revolution in the case of hovering flight, allows to perform circulation measurement by only considering the variation of the tangential velocity componant with the phase on the upper and lower side of the rotating plane.

Four rotors of different tips shape plan forms have been tested (rectangular, parabolic, tapered and swept) and compared to calculations in the case of rectangulàr and tapered tips. Moreover, the measurements of the induced axial velocity at the rotating plane have given, by use of Kutta-Joukowski formula and 2.D lift and drag distribution, the radial loading distribution compared to the one directly deduced from the circulation measurements.

2. EXPERIMENTAL SET-UP AND TEST CONDITIONS.

The Rotor

A model-scale rotor, 1.5 m in diameter was used in hover for this study in the open test chamber of a wind tunnel. Four interchangeable blades were tested (see Fig.1 for geometric blade properties). The tip velocity was fixed at 107 m/s in all experiments. Geometrical rotor properties and test operating conditions are summarized in table 1.

Table 1

Rotor diameter	: 1.5 m
Blade chord	: 0.05 m
Airfoil	: OA209
Blade twist (linear)	: - 8°.3
Number of blades	: $2 \leqslant b \leqslant 4$
Coning angle	: ≃ 2.5°
Root cutout	: 0.22R
Rotor speed Ω	: 143 rad/s
Tip speed	: 107 m/s

The laser velocimeter (L.V.)

The L.V. is equiped for 2.D measurements and operates in backscattering mode (focal lenght of frontal lens of, 1.8 m). Reverse flow measurements are made possible by the adjonction of a bragg-cell. A traversing system supporting the L.V. allows to displace the focal volume along radial, tangential and axial directions to obtain the axial and chordwise velocity components used for calculating the circulation as described below.

Photomultipliers output were analysed by counters and stored through an interface in a microcomputer HP9845 B. The L.V. operated in continuous light in such a way that all velocity informations were recorded during N rotations of the rotor. The phase rotation of each measurement was known by means of an angular counter and the corresponding position of the blade by means of a photo cell. Figure 2 presents the L.V. system. For each phase angle varying from 0 to $2\Pi/b$ an histogram made on 200 samples of the stored velocities was realized resulting in the instantaneous mean velocity value. An histogram example is presented in figure 3.

3. DEFINITION OF THE TWO CONTOURS.

3.1. Contour at a fixed phase angle. Method 1

In order to determine the circulation around a profile of the blade, a rectangular box ABCD was defined, surrounding as close as possible the profile (see figure below).

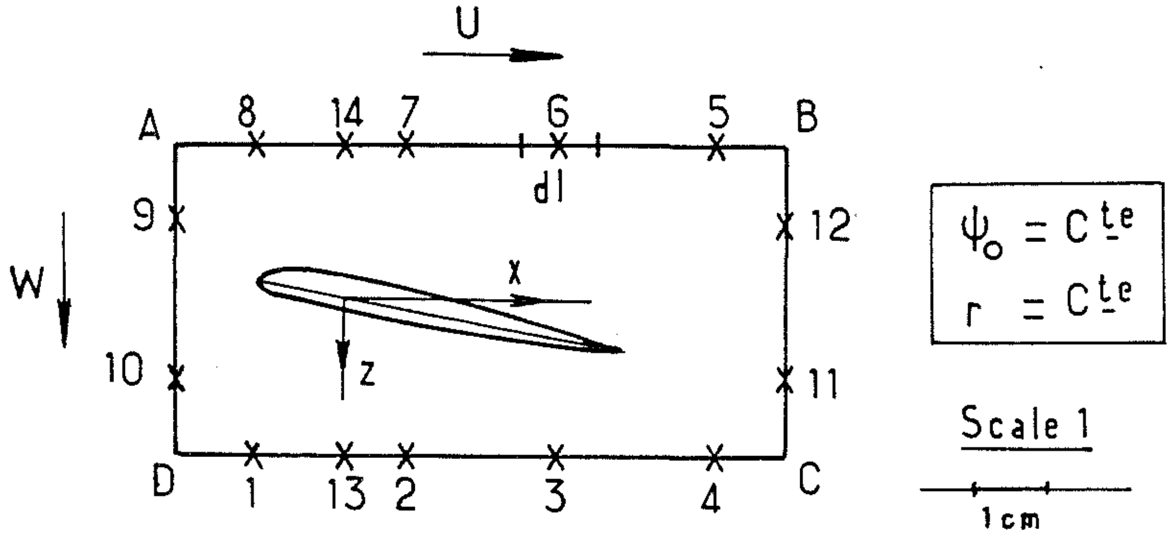

The focal volume was displaced along ABCD and in each point (1,2,3,4, 13) (5,6,7,8,14) and (9,10) (11,12) the variations with Ψ of U and W componants respectively were measured. Figure 4 shows as an example at r/R = 0.8 the distribution of U with ψ at points 13 and 14 (upper part of the figure) and W at points 9 and 10 (lower part of the figure). In our test conditions, the position of the airfoil just inside the box corresponded to a phase Ψ_o = 9.36°. The circulation is then deduced from the values of U and W at points 1 to 14 and at $\Psi = \Psi_o$ by the formula :

$$\Gamma = \sum_{\substack{AB\ (\Psi_o)\\ CD}} U_n\, dl_n + \sum_{\substack{AD\ (\Psi_o)\\ BC}} W_n\, dl_n$$

The incertitude on the profile position inside the box due to the precision of the angular counter is about 0.36° in Ψ resulting in an incertitude of 4 mm in x direction at r = R.

Moreover, it can be observed on figure 4 that the presence of the profile induces pics of velocity at phase $\Psi \simeq \Psi_o$ as excepted. When the profile is far from the measurement point ($\Psi = \frac{1}{2}\,\frac{2\Pi}{b} + 9°.36 \simeq 55°$), the - velocities keep a lower constant value corresponding to the inflow between two blades.

3.2. Contour made on $\frac{2\Pi}{b}$ phase variation. Method 2

The calculation of circulation presented in § 3.1 may introduce an important incertitude because of the small number of measurements along branches AD and BC. The L.V. operating in continuous light, strong reflexions on the blades occur when the focal volume is located between points 11 and 12, and 9 and 10; it was the reason why no measurements could be realized in these regions. But, owing to the symmetry of the flow with phase angle variation of 2 Π/b, if the branches AD and BC belonging to the same radius are separated by an angle of 2 Π/b, the componant W along AD will be the same as along BC.

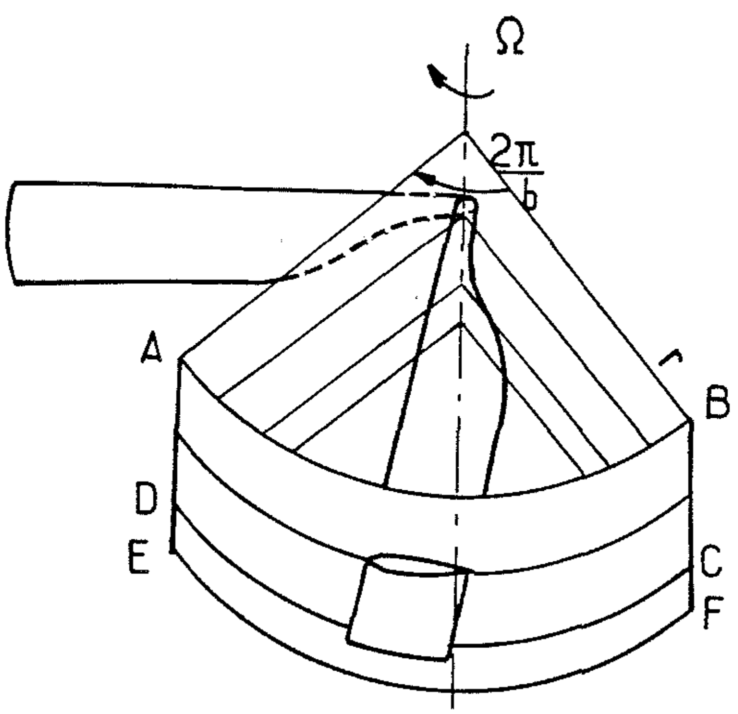

The contribution of branch DA to circulation will be balanced by the circulation along BC. The circulation along the contour ABCD defined in the figure above is then reduced to circulation along AB and CD. Moreover, it can be noticed that the variation with Ψ of the U component in any point of AB *may represent for a fixed position of the wing the variation of U along* AB when replacing ψ by $r\psi$. It will be noted in figure 5 that the velocity profiles U and W measured in different points of the contour are only phase lagged.

When plotting on the same graph the variations of U_{AB} and U_{DC} versus $r\psi$ (U_{AB} and U_{DC} are measured at the same radius and the same vertical plane, on th upper and lower side of the rotating plane), the circulation along ABCD can be written :

$$\Gamma_{ABCD} = \int_{AB} U_{AB}\, d\ell - \int_{DC} U_{DC}\, d\ell + \underbrace{\int_{DA} W\, d\ell - \int_{CB} W d\ell}_{o}$$

or $$\Gamma_{ABCD} = \int_{o}^{2\,\Pi/b} (U_{AB} - U_{DC})\, r d\psi$$

The circulation can then be calculated as the surface comprised between the two curves U_{AB} and U_{DC}, as shown below.

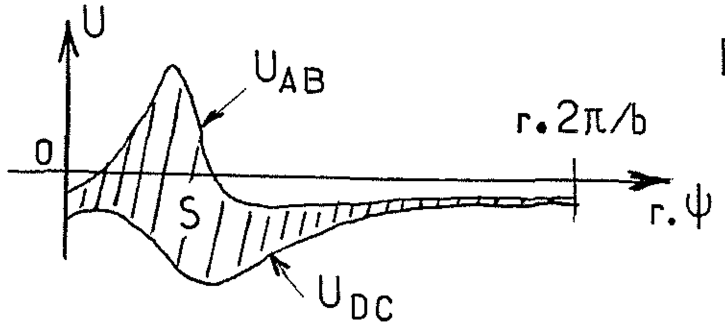

$\Gamma_{ABCD} = S$

REMARK. Due to the contraction of the wake, some vorticity of intensity Γ_E coming from preceding blades can be present in the contour between the plane of rotation and branch DC. If Γ is the circulation just around the blade profile at *r*, then *:* $\Gamma_{ABCD} = \Gamma + \Gamma_E$ or $\Gamma = \Gamma_{ABCD} - \Gamma_E$. Γ_E has been evaluated by considering the circulation around a contour DCFE non including the profile. This circulation is found by integrating as previously shown $U_{DC} - U_{EF}$ along $r\,\psi$. The variations of U_{DC} and U_{EF} is shown as an example on figure 6 for r/R = 0.95. The circulation concerns a contour of e in width and this case (e = 1 cm) $\Gamma_{DCFE} = 0.05\,\Gamma_{ABCD}$. A linear distribution of vorticity may be assumed just below the rotating plane and Γ_E may be written : $\Gamma_E = \Gamma_{DCFE} \times \frac{L}{e}$ where L is the distance between the rotating plane and the branch DC. For the four tested rotors, circulation Γ_{ABCD} was measured at different $\frac{r}{R}$ (0.3; 0.4; 0.5; 0.6; 0.7; 0.75; 0.8; 0.85; 0.9; 0.95; 1) and corrected according to the above method to obtain Γ around the profile.

4. RESULTS

The radial distribution circulations as obtained by the two methods previously described have been compared. As an example, figure 7, relative to rotor 7, presents the result of the comparison; the agreement is relatively good for $\frac{r}{R} < 0,7$, although in the tip region ($0.8 \leqslant r/R \leqslant 1$) discrepancies appear, with scattered data. When experimental values are compared to results given by a free wake analysis code (5) it can be noticed that the results deduced from $\frac{2\Pi}{b}$ r contour (method n°2) are in better agreement that those deduced from ψ = Cte contour (method n°1) and fit pretty well calculations except in the region of the pic circulation where experiments predict a maximum more inboard and less intense. In the same figure have also been plotted the values of circulation deduced from Kutta-Joukowski formula and 2-D aerodynamic coefficients of blade airfoils. The incidence is calculated from the measurements of induced velocities. It can be seen in figure 7 that these values of circulation are underestimated all along the blade compared to calculation. Moreover, it has been possible to compare the traction directly measured by strain gages to the ones obtained by integration of Γ along the blade. The traction measured is T_m = 195 N, calculated with Γ from method 1 T_1 = 138 N, from method 2 T_2 = 190 N and from Kutta-Joukowski and 2-D aerodynamics coefficients T_{K-J} = 135 N. These results clearly indicate that method 2 is the more suitable to carry out a realistic distribution of circulation better than others when refering to experimental traction of the rotor. It is also interesting to note that this method is less time consuming (no displacement of the focal volume around the profile is needed). Hence, the results presented below have been obtained by method 2.

Figure 8 concerns rotor 7 at a lower general pitch angle ($\theta_{0.75} = 8°$) and Figure 9 at a lower number of blades (b = 2). The lift coefficient distribution with r/R has also been plotted on the figures. The comparison with calculations shows the same tendency than previously described : the experimental pic of circulation is found more inboard.

Figure 10 is relative to rotor 6. The calculation code is inoperative in this case and only experiments are presented as in figure 12 which concerns swept tip plan-form. In these two cases two maxima of circulation appear : a first at about $r/R \simeq 0.75$ and a second of high intensity at $r/R \simeq 0.9$.

Finally, Figure 11 presents the results obtained relative to rotor 5 (tapered plan-form). Comparison has been made to calculations and it is interesting to remark the good agreement of experimental and calculated distribution concerning the location of two maxima at $r/R = 0.75$ and $r/R = 0.95$. Quantitative comparisons are also pretty good.

The tractions deduced from circulation distributions (method 2) have been calculated for all tested rotors and compared to experimental value. The results are presented in table 2.

Table 2

N° Rotor	b	$\theta_{0.75}$	Measured	T(N) Deduced from Method 2
7	2	10	99	110
7	4	10	195	190
7	4	8	150	148
6	4	8	150	155
5	4	8	155	160
4	4	8	155	152

5. CONCLUDING REMARKS

A laser-velocimeter was shown to be a suitable instrument for determining the radial distribution circulation of a rotor in hover. The method using a $\frac{2\Pi}{b}$ r contour has been preferred to a contour at ψ = Cte around the profile because more precise and less time consuming. Radial distribution circulation have been carried out for different tip plan-shapes (parabolic, tapered and swept) showing the existence of two maxima in the distribution of circulation. Comparison to a free wake calculation code and to direct measurements of traction has indicated that the $\frac{2\pi}{b}\Gamma$ contour method was more operative than the use of Kutta-Joukowski formula associated to the 2-D aerodynamics coefficients of blade airfoils.

The results have also shown that the L.V. was a powerful tool for designing tip plan-form shapes with reference to tip distribution circulation.

ACKNOWLEDGEMENTS. We gratefully acknowledge the support provided by the Direction des Recherches, Etudes et Techniques, under Grant D.R.E.T. N° 82/432.

REFERENCES.

1. Ninth European Rotorcraft Forum
Papers N°2, 14, 20, STRESA, Italy, September 1983.

2. A.J. LANDGREBE
"An Analytical and Experimental Investigation of Helicopter Rotor Hover Performance and Wake Geometry Characteristics". USAAMRDL Technical Report 71-24, Eustis Directorate, U.S. Army Air Mobility Research and Development Laboratory, Fort Eustis, Va., June 1971.

3. C. MARESCA, M. NSI MBA, D. FAVIER
"Prédiction et vérification expérimentale du champ des vitesses d'un rotor en vol stationnaire". Prédiction of Aerodynamic Loads on Rotorcraft AGARD-CP-334, U.K., LONDON, May 1982.

4. J.D. BALLARD, K.L. ORLOFF
"Effect of Tip Shape on Blade Loading Characteristics and Wake Geometry for a Two-Bladed Rotor in Hover". Journal of the American Helicopter Society, January 1980.

5. J.M. POURADIER, E. HOROWITZ
"Aerodynamic Study of a Hovering Rotor". Proceeding of 6th European Rotorcraft and Powered Lift Forum, BRISTOL, September 1980.

Rotor number	Twist	Planform and tip shapes	Profile
4	-8,3°	α = 60°, a	OA 209
5	-8,3°	b, d	OA 209
6	-8,3°	0,95 R, R	OA 209
7	-8,3°		OA 209

a = 0,15c
b = 0,25c
d = 0,60c

Fig. 1

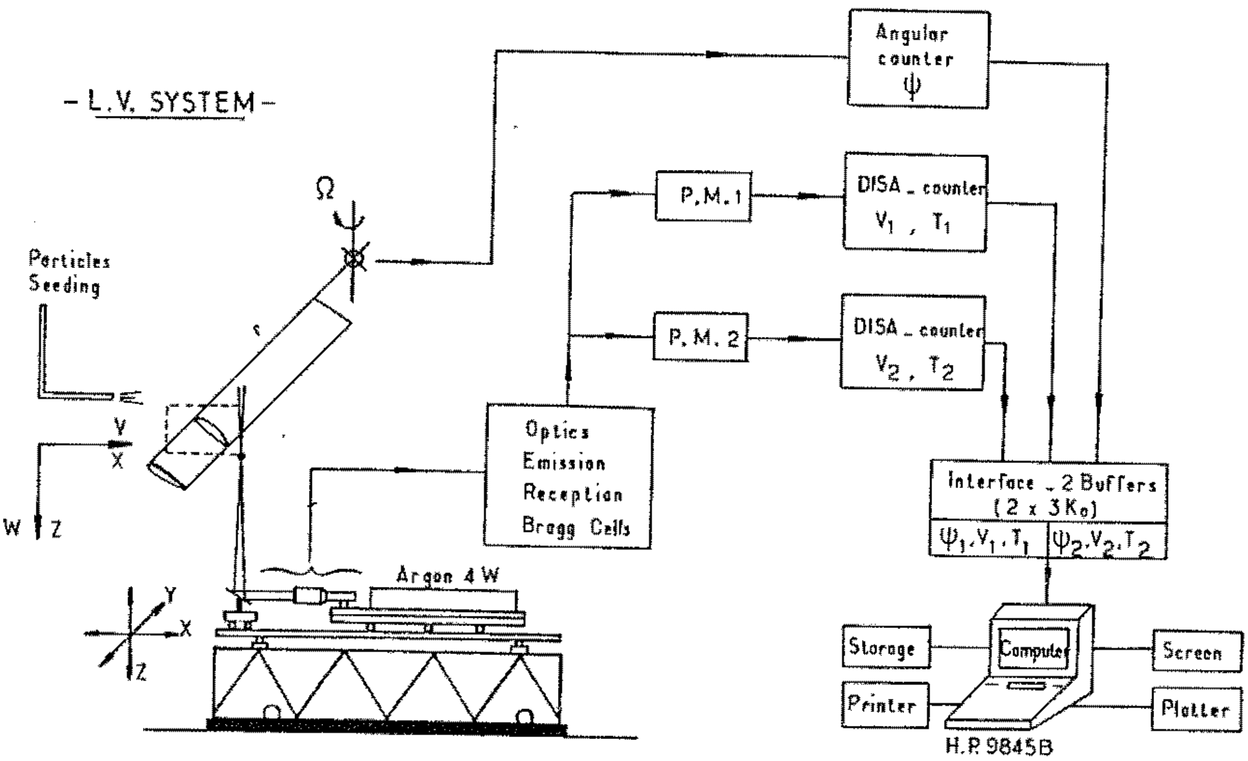

Fig. 2

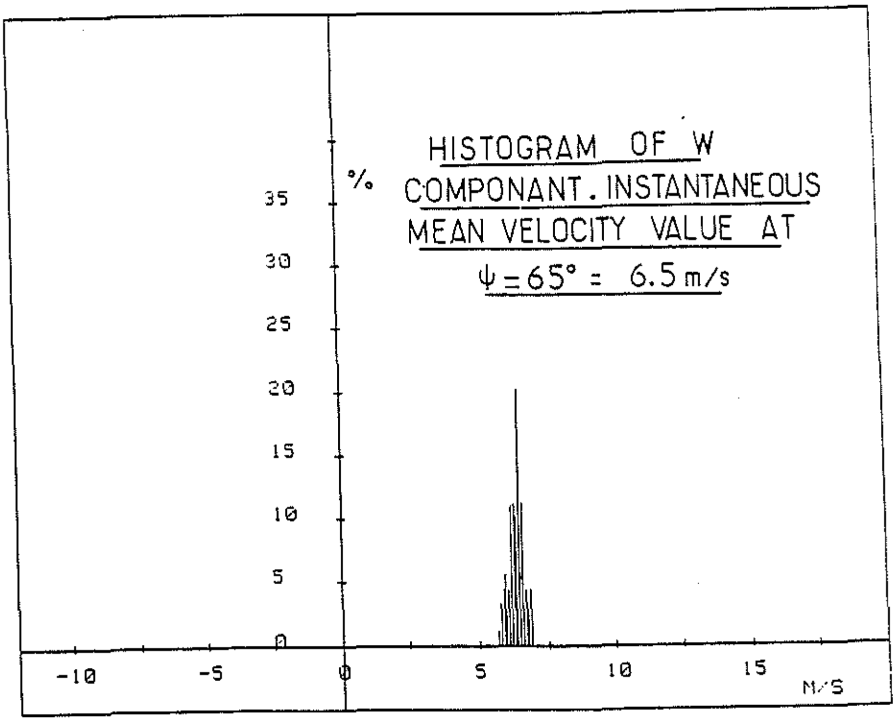

Fig. 3

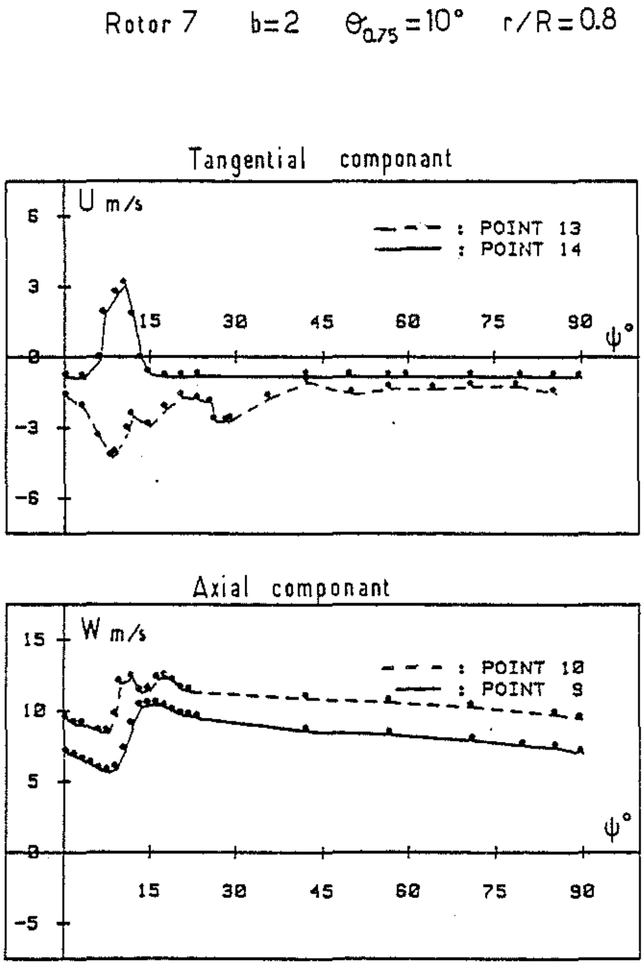

DISTRIBUTION WITH ψ OF INDUCED VELOCITIES

Fig. 4

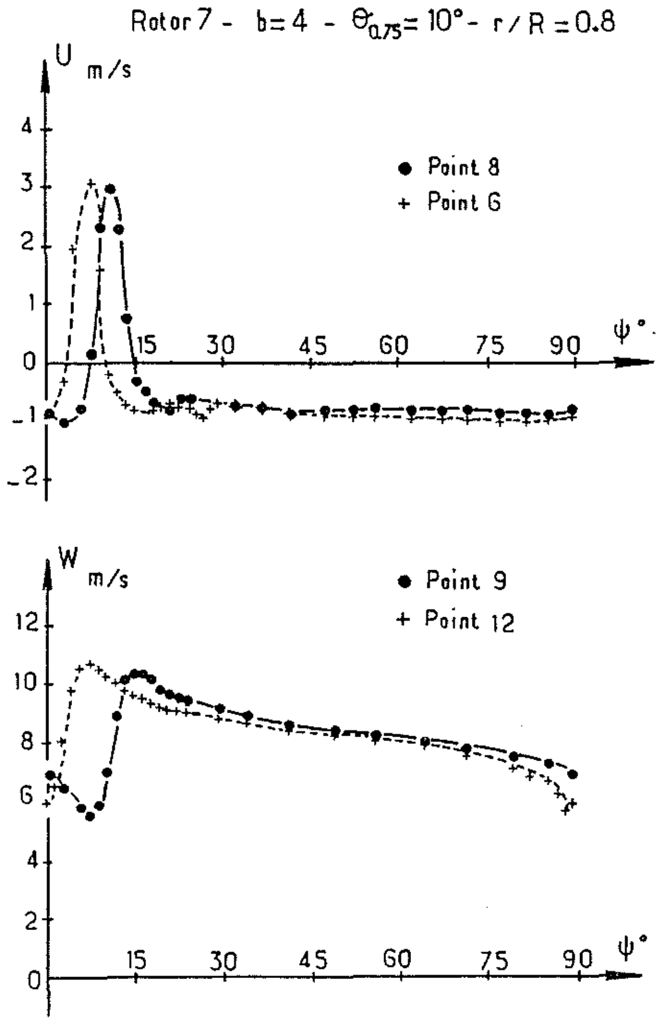

PHASE LAG ON VELOCITIES IN DIFFERENT POINT MEASUREMENTS

Fig. 5

Rotor 7 - b=4 - $\theta_{0.75}$=10° - r/R = 0.9

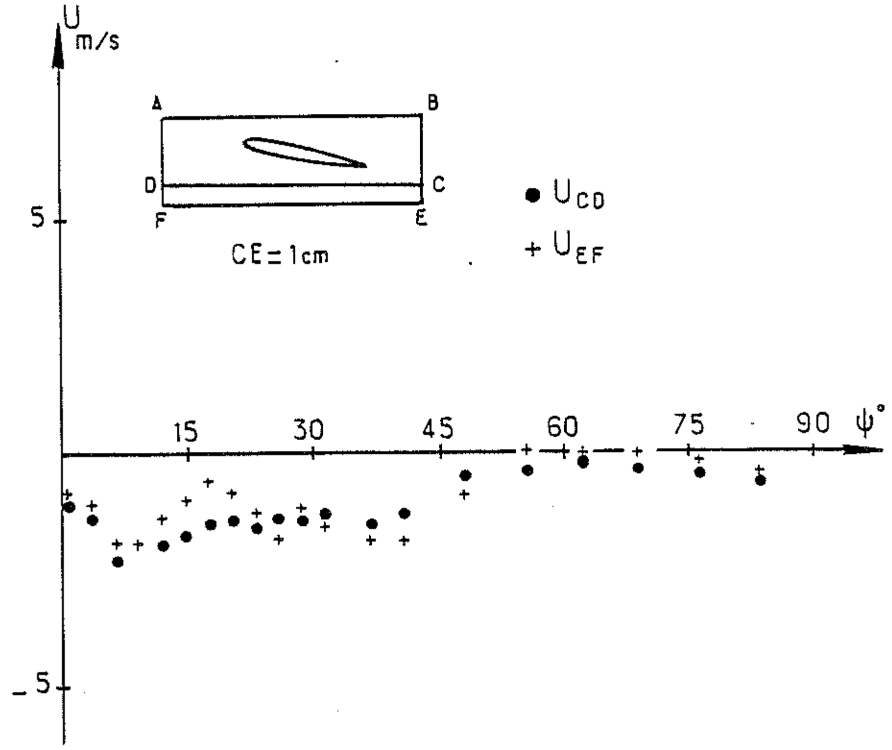

Fig. 6

VARIATION OF U WITH AXIAL DISTANCE

Rotor 7 - b=4 - $\theta_{0.75}$= 10°

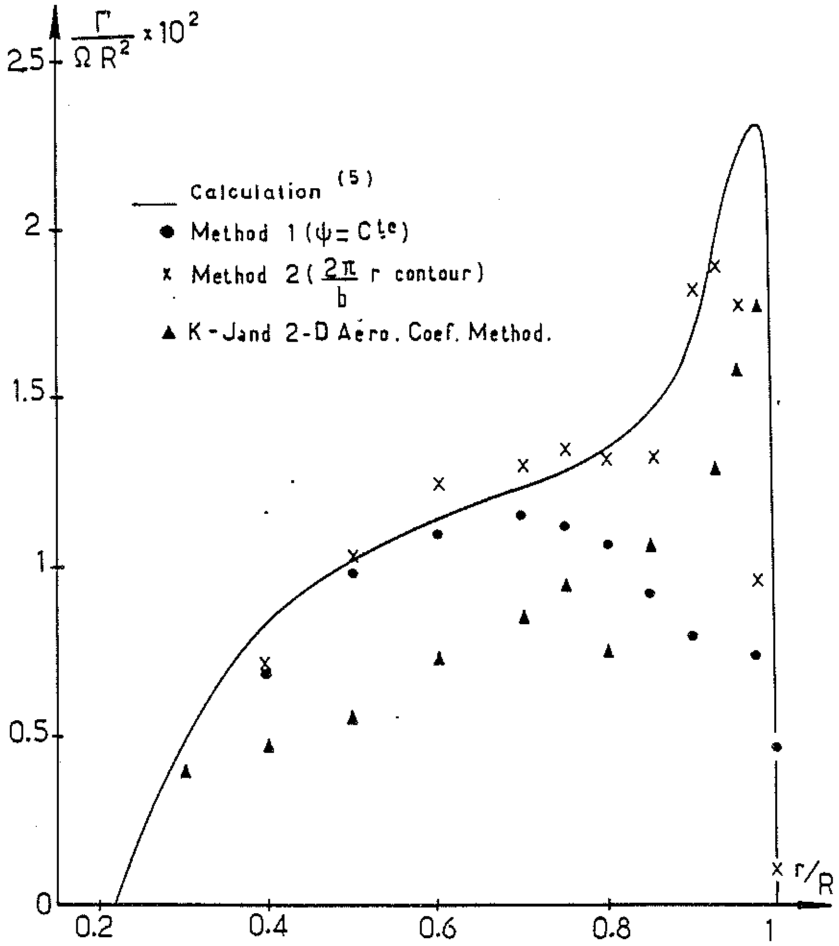

Fig. 7

RADIAL DISTRIBUTION OF CIRCULATION ALONG THE BLADE

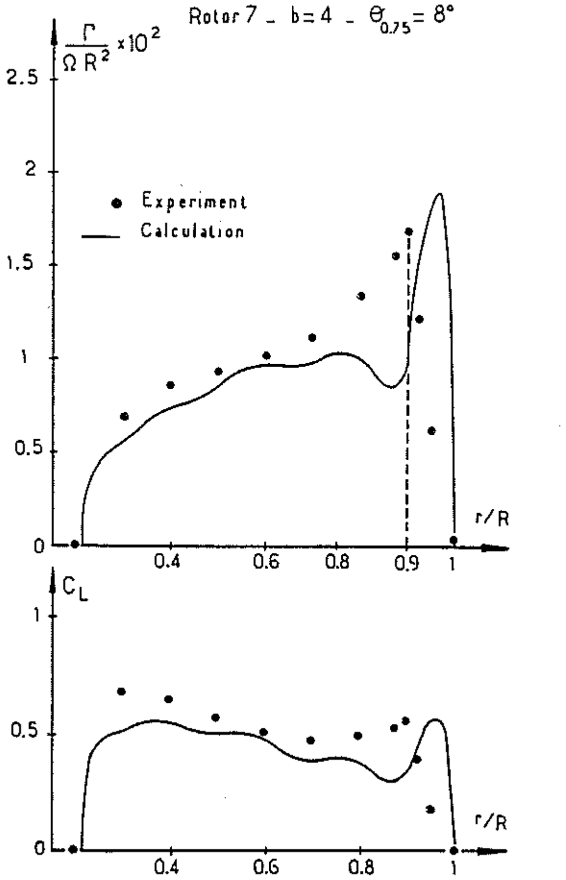

RADIAL DISTRIBUTION OF CIRCULATION
AND LIFT COEFFICIENT ALONG THE BLADE

Fig. 8

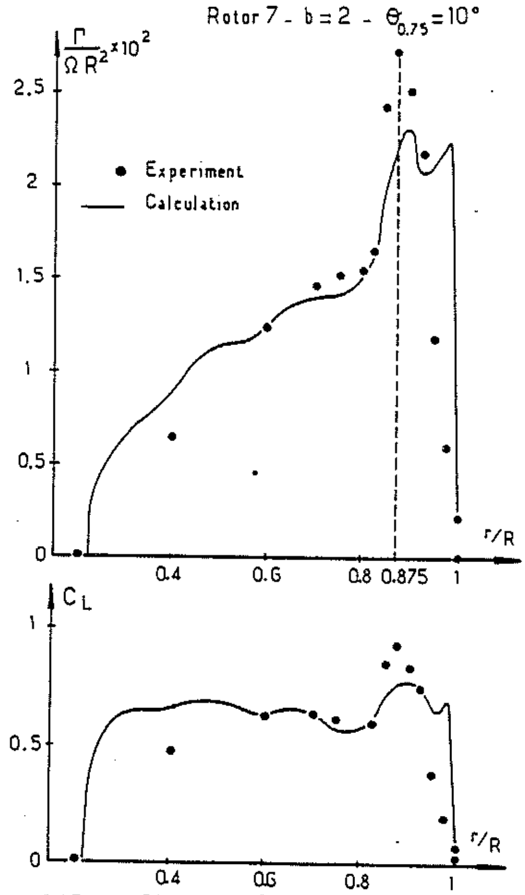

RADIAL DISTRIBUTION OF CIRCULATION
AND LIFT COEFFICIENT ALONG THE BLADE

Fig. 9

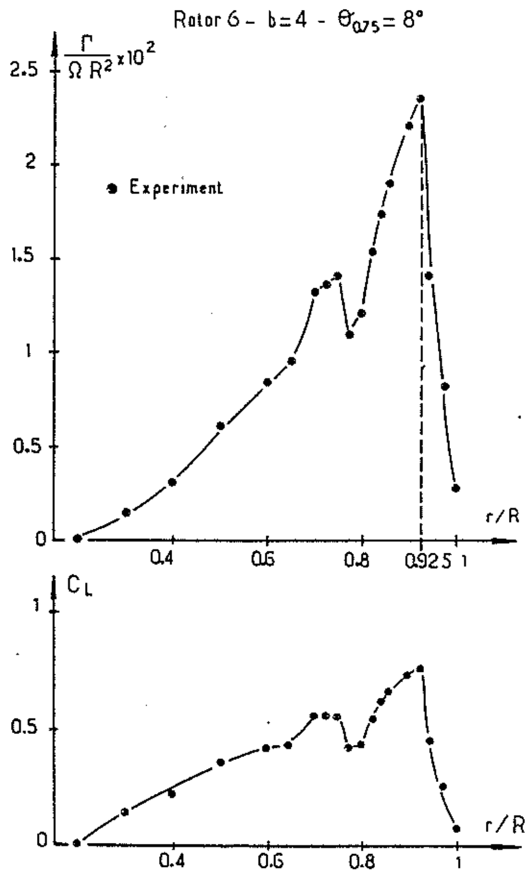

RADIAL DISTRIBUTION OF CIRCULATION
AND LIFT COEFFICIENT ALONG THE BLADE

Fig. 10

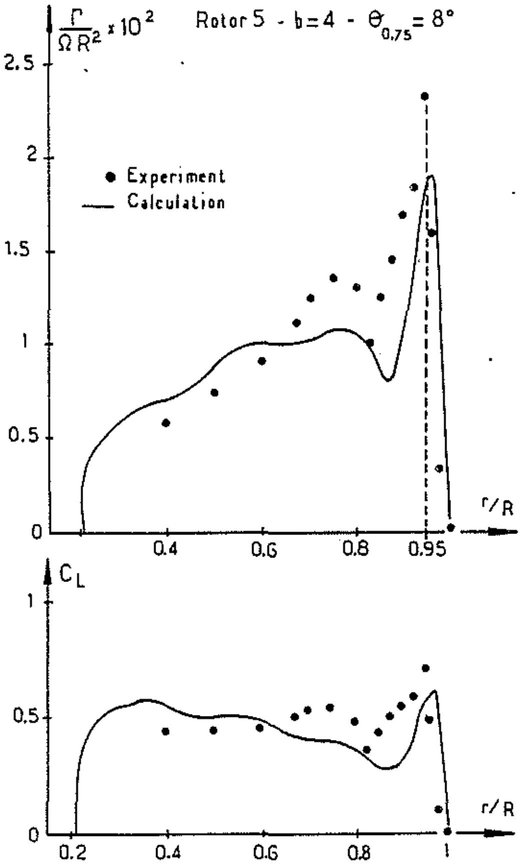

RADIAL DISTRIBUTION OF CIRCULATION AND LIFT COEFFICIENT ALONG THE BLADE

Fig. 11

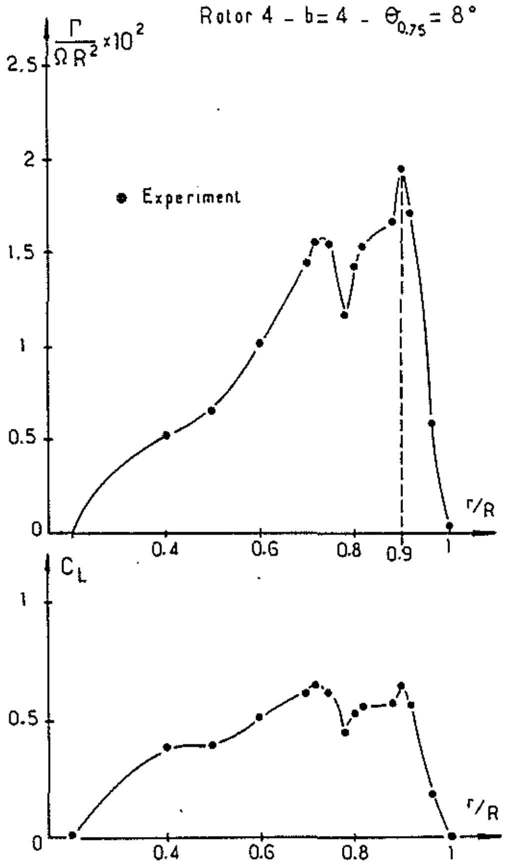

RADIAL DISTRIBUTION OF CIRCULATION AND LIFT COEFFICIENT ALONG THE BLADE

Fig. 12